A Discrete-Components Impulse-Radio Ultrawide-Band (IR-UWB) Transmitter

James Colli-Vignarelli and Catherine Dehollain

***Abstract*—We describe an impulse-radio ultra-wideband (IR-UWB) transmitter made with off-the-shelf discrete components. It was initially designed to be used in a UWB testbed for measurement and algorithm validation purposes. There already exist several versions of an IR-UWB transmitter, but many of them are made with custom designed integrated chips. For this reason, it is very difficult for anyone other than their designers to test and measure with the same material. We describe all the information the readers would need to build their own IR-UWB transmitter.**

***Index Terms*—Discrete components, impulse-radio (IR), transmitter, ultra-wideband (UWB).**

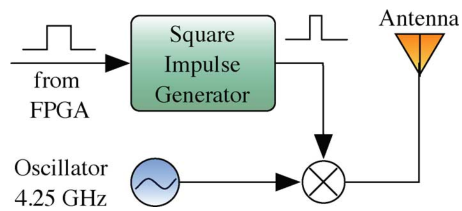

Fig. 1. Overview of the transmitter. The transmitter is made around a PLL synthesizer that creates the 4.25-GHz sine wave. This signal is switched on during about 3 ns by the mixer driven by the impulse generator. This makes the radiated signal to have a UWB spectrum. These impulses are produced from the bit stream of the FPGA board (not shown in figure) every time a logic one is sent. The duration of a bit from the FPGA (chip time) is 6 ns. The antenna does not belong to the transmitter and is connected outside.

I. INTRODUCTION

IMPULSE-RADIO ultra-wideband (IR-UWB) technology is a growing technology that combines several facilities such as high data-rate transmission, low-power consumption, and localization. Today, one of the main challenges is to provide new protocols and signal-processing algorithms that allow for concurrent IR-UWB transmissions and synchronization in mobile networks. More precisely, there are algorithms on synchronization or localization for which an experimental validation is required in order to prove the concept and to improve their performance by considering the obtained results. For example, the validity of the synchronization algorithms described in [1] is theoretically proven by simulations and mathematical derivation, but there is a need to experimentally demonstrate and validate them in realistic scenarios such as the near-far one. For this purpose, a complete IR-UWB testbed was realized, as described in [1], which gives the desired experimental validation of these algorithms. Another example is given in [2], where the same testbed is used to demonstrate and validate a new algorithm on ultra-wideband (UWB) localization.

The UWB transmitter described here is a fundamental part of this testbed. As this circuit is specially intended for communication research community, we focus on simplicity and availability of required components rather than pure technologic performance. The objective is thus to make it simple, generic, and to avoid the need for the high-level background and technical infrastructure required in integrated circuit (IC) design. In order to make our testbed reproducible at reasonable costs, we chose to build it with off-the-shelf discrete components. There are no constraints on the power consumption. The 4.0–4.5-GHz band was chosen from the allowed UWB band [3] because there is no other transmission system that sends signals into it. Thanks to its generic architecture, it is easy to modify the transmitter in order to work in another frequency band or with a wider bandwidth, depending on the needs of the users.

Manuscript received March 26, 2010; revised December 20, 2010; accepted January 17, 2011. Date of publication March 10, 2011; date of current version April 08, 2011. This work was supported in part by the National Competence Center in Research on Mobile Information and Communication Systems (NCCR-MICS), a center supported by the Swiss National Science Foundation under Grant 5005-67322.

The authors are with the Sciences et Techniques de l'Ingénieur–Radio Frequency Integrated Circuit (STI-RFIC) Group, Ecole Polytechnique Fédérale de Lausanne, Lausanne CH-1015, Switzerland (e-mail: james.colli-vignarelli@epfl.ch; catherine.dehollain@epfl.ch).

Color versions of one or more of the figures in this paper are available online at http://ieeexplore.ieee.org.

Digital Object Identifier 10.1109/TMTT.2011.2114194

II. ARCHITECTURE OF THE TRANSMITTER

A. Topology of the Transmitter

For robustness and flexibility, our UWB transmitter is based on a classic architecture (see, e.g., [4]–[6]), as shown in Fig. 1. Readers interested in making a testbed with transmitters based on other architectures that require very specific components such as step-recovery diodes can see [7] and [8] for examples. An oscillator based on a phase-locked loop (PLL) synthesizer produces a 4.25-GHz sine wave that is switched on during about 3 ns. The duration of the driving impulse is adjustable, as explained later. The mixer, when driven by a digital impulse, behaves like a switch. The square impulse generator is driven by a rectangular signal coming from a field-programmable gate array (FPGA) and converts each incoming digital impulse into a fast switching impulse. The FPGA board is the model AC-240 from Aquiris and belongs to the specifications. The maximal clock frequency of the FPGA is 166 MHz; hence, the chip time (the duration of a bit, see [1]) is limited to a minimum of 6 ns. The output UWB signal is sent to an omnidirectionnal antenna (not described in this paper, but in [9]) that has a 50-Ω impedance.

B. Analysis of the Effect of Pulse Duration

This section describes the relation between a sinusoidal pulse of duration Tp and its spectrum bandwidth [10], as done by using the above architecture. By assuming a perfect rectangular impulse window centered in $t = 0$ (for easier further developments), the output signal is described in the time domain by

$$P_{\mathrm{UWB}}(t) = W_{Tp}(t) \cdot A \cdot \sin(2\pi f_0 t)$$

where

$$W_{Tp}(t) = \begin{cases} 1, & \text{if } -\dfrac{Tp}{2} \leq t \leq \dfrac{Tp}{2} \\ 0, & \text{else} \end{cases}$$

and A is the amplitude in volts. The idea here is to calculate the Fourier transform of such a pulse and to determine for which value of Tp its spectrum fulfills the UWB requirements. By doing this, we obtain a fundamental relation between the pulse duration and the spectrum bandwidth, as seen hereafter. Let

$$F(f) = \mathfrak{F}(P_{\mathrm{UWB}}(t)) = \int_{-\infty}^{\infty} P_{\mathrm{UWB}}(t) \cdot e^{-j2\pi ft} dt$$

be the Fourrier transform of this impulse. By applying Euler's identity and changing integration boundaries, we obtain

$$F(f) = A \cdot \int_{-\frac{Tp}{2}}^{\frac{Tp}{2}} \sin(2\pi f_0 t)[\cos(-2\pi ft) + j \sin(-2\pi ft)]\, dt.$$

After elementary trigonometric and calculus transformation, the integral value is given by

$$\begin{aligned} F(f) &= jA \left(\frac{\sin(\pi(f_0+f)Tp)}{2\pi(f_0+f)} - \frac{\sin(\pi(f_0-f)Tp)}{2\pi(f_0-f)} \right) \\ &= jA\frac{Tp}{2} \left(\mathrm{sinc}(\pi(f_0+f)Tp) - \mathrm{sinc}(\pi(f_0-f)Tp) \right). \end{aligned}$$

The spectrum is maximum in f_0 with a very good approximation and its value at this frequency is given by

$$F(f_0) = jA\frac{Tp}{2}(\mathrm{sinc}(2\pi f_0 Tp) - 1)$$

assuming that $\mathrm{sinc}(\pi(f_0+f)Tp) \ll \mathrm{sinc}(\pi(f_0-f)Tp)$. The frequency f_0 corresponds to the central frequency of the UWB spectrum, and thus is the frequency delivered by the sine-wave oscillator previously described. By normalizing the spectrum with its maximum value, we define the attenuation as

$$\begin{aligned} A(f) &= \frac{F(f)}{F(f_0)} \\ &= \frac{\mathrm{sinc}(\pi(f_0+f)Tp) - \mathrm{sinc}(\pi(f_0-f)Tp)}{\mathrm{sinc}(2\pi f_0 Tp) - 1}. \end{aligned} \tag{1}$$

Since in the UWB domain, the corner frequency is defined at -10 dB of the maximum value instead of -3 dB, as done in usual applications, we have to look for values of f such that $A(f) = \sqrt{0.1} = 0.3162$. The square root is used because we consider voltage instead of power. For this purpose, we consider the fundamental wave relation $f_0 \cdot T_0 = 1$ and let

$$\begin{aligned} Tp &= \alpha \cdot T_0 \\ f &= \beta \cdot f_0 = f_\beta \end{aligned}$$

where α and β are dimensionless scaling values for the time and frequency, respectively. By inserting this into (1), we obtain

$$A(f_\beta) = \frac{\mathrm{sinc}(\pi(1+\beta)\alpha) - \mathrm{sinc}(\pi(1-\beta)\alpha)}{\mathrm{sinc}(2\pi\alpha) - 1}. \tag{2}$$

The bandwidth B is then simply defined as $B = 2f_0(1-\beta)$ and we thus have the following fundamental relation:

$$B \cdot Tp = 2(1-\beta)\alpha = K \tag{3}$$

where K is a parameter that depends on the quality factor $Q = (f_0)/(B) = (1)/(2(1-\beta))$. This dependency between K and Q is better understood by noting that β depends on α from (2).

C. Numeric Application and Design Procedure

The IR-UWB transmitter described in this paper works from 4.0 to 4.5 GHz so $B = 0.5$ GHz and $f_0 = 4.25$ GHz (and thus, $T_0 = 0.2353$ ns). Thus, β is given by

$$\beta = 1 - \frac{1}{2Q} = 1 - \frac{B}{2f_0} = 1 - \frac{0.5}{2 \cdot 4.25} = 0.9412.$$

We then calculate α by solving numerically—e.g., by iteration—(2) with $A(f) = 0.3162$. We find $\alpha = 12.46$. The pulse duration is given by

$$Tp = \alpha \cdot T_0 = 12.46 \cdot 0.2353 \text{ ns} = 2.932 \text{ ns}$$

and the fundamental relation parameter is

$$K = B \cdot Tp = 2(1-\beta)\alpha = 2(1-0.9412) \cdot 12.46 = 1.47 \tag{4}$$

with $Q = 8.5$. In practice, the pulse duration is about 10% greater in order to compensate the envelope that is not perfectly square, but trapezoidal (due to the balun) and the spectrum that would consequently be too wide.

III. Schematic of the Transmitter

A. Overview of the Circuit

The complete schematic of the UWB transmitter is shown in Fig. 2. Many decoupling capacitors are required because almost every IC has its own power supply voltage; these voltages are obtained by inserting resistors between their corresponding circuits and the main power supply. This is possible because the

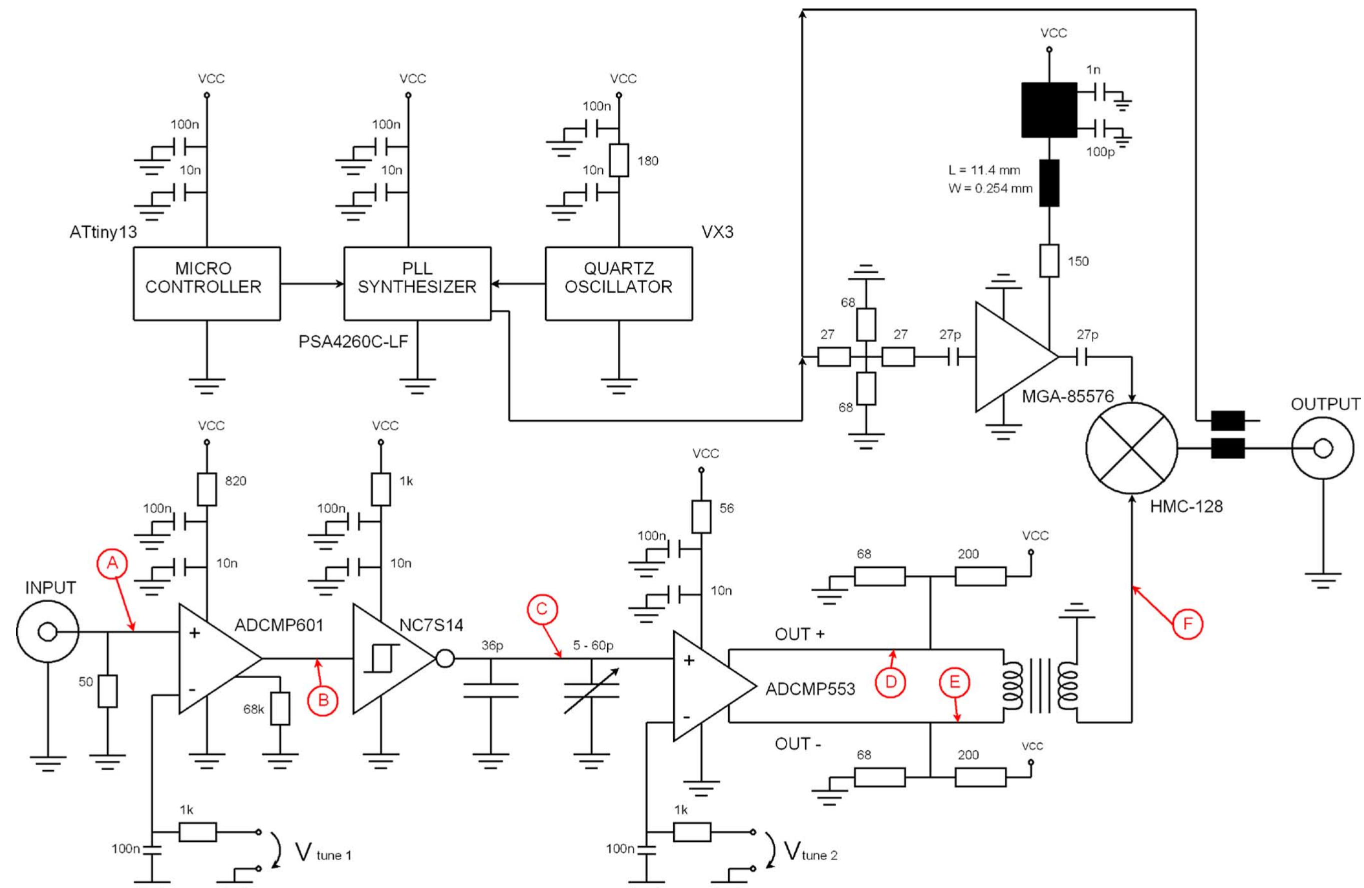

Fig. 2. Complete schematic of the UWB transmitter. The upper part is dedicated to the PLL synthesizer and the lower part is dedicated to the square impulse generator. The mixer, on the right, combines both signals; the UWB signal goes to the antenna (outside the box) through the SMA connector OUTPUT. The coupled transmission line at output represents the line of the coupler that is used for correcting the feed-throught of the mixer (see Section III-D and Fig. 5). The signal for an impulse arrives in A (SMA connector INPUT) and is shaped by the first comparator in B at level V_{tune1}. A Schmitt-trigger inverter, loaded with a variable capacitive load gives a kind of triangle signal in C. A fast comparator then makes the short impulse by triggering at V_{tune2} in D and E. As the fast comparator is made in PECL, the output is balanced and needs a dc voltage of 1.3 V in order to ensure the correct bias and to set the corresponding logic values voltages. A balun transformer is used to produce the unbalanced and dc free signal for driving the mixer in F. See Fig. 3 for the corresponding signals.

circuits have a constant current consumption (we can neglect current transients, thanks to the 10-nF decoupling capacitors).

B. PLL Synthesizer

The PLL synthesizer is a classic circuit without any difficult design considerations. It uses a 50-MHz quartz reference for better frequency precision and a microcontroller for setting the divider parameters. According to the manufacturer, the output sine wave needs to be decoupled by a resistive attenuator and then to be amplified in order to reach the power level required at the local oscillator (LO) input of the mixer; this is needed because the voltage-controlled oscillator (VCO) is very sensitive to any mismatch that can occur on the load. There is a switch for decoupling the PLL circuit when programming the microcontroller.

C. Description of the Square Impulse Generator

The square impulse generator takes the pulse coming from the FPGA board and reshapes it in order to obtain a very short impulse of approximately 3 ns that drives the mixer. As the FPGA board connections have poor impedance-matching characteristics (point A in Fig. 2), the signal first has to be squared by a comparator in order to obtain the original rectangular signal (point B). The comparator triggers at V_{tune1} level and a Schmitt-trigger inverter is then used as a buffer for driving a capacitive load (point C), which produces a triangular signal that is made of arcs of exponentials. The capacitance is variable, and this is how the pulse duration is adjusted (in conjunction with V_{tune2}). A fast positive emitter coupled logic (PECL)-based comparator triggers this signal at the V_{tune2} level to produce the short impulse (points D and E). As the PECL logic defines the low level at 1.3 V and the high level at 2 V and uses balanced signals, a balun transformer is required to obtain the same signal with unbalanced polarity and no dc voltage level. In the schematic, the dc voltage is obtained with a resistive divider, which gives 1.3 V with a 50-Ω impedance. As the balun, like the divider, has an impedance of 50 Ω, the total impedance seen by the output of the PECL is 25 Ω, which is in the driving range of the circuit.

D. Mixer and Correction of the Feed-Through

When we designed the first prototypes of the UWB transmitter, there was a high feed-through from the mixer between the local PLL synthesizer and the RF UWB output. This feed-through made a high peak (measured at about -30 dBm) in

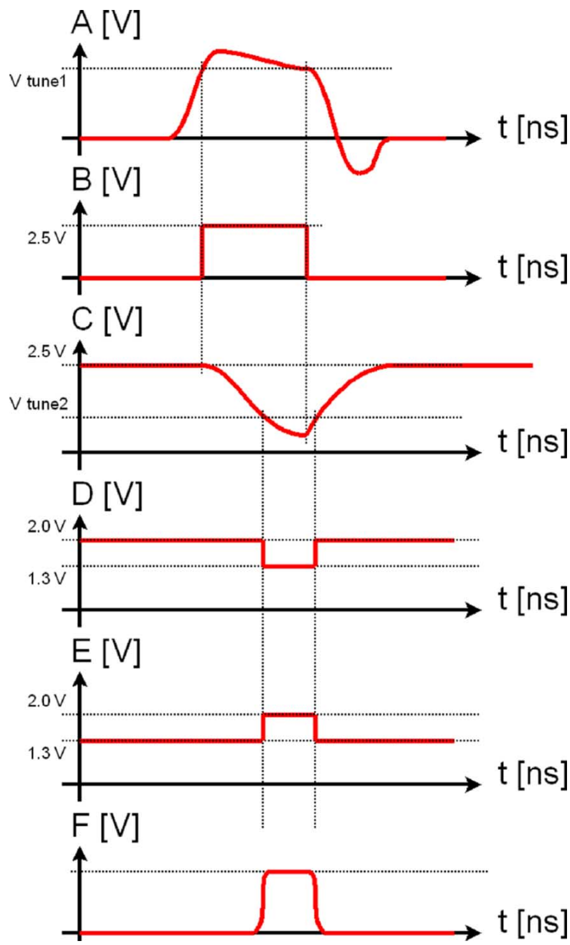

Fig. 3. Signals involved into the square impulse generator circuit. See Fig. 2 for the corresponding circuit.

the spectrum at 4.25 GHz, which made the transmitter initially not compliant with the FCC regulations. To solve this, we use a transmission line coupler in order to create destructive interference between the oscillator and the RF output (see Fig. 2). Physically, the coupler is simply made with a wire soldered at one end of the resistive attenuator pad and it passes above the mixer and the RF output track while its other end stays in the air. By experimentally giving it by hand an appropriate shape (see Fig. 5 for more detail), it is possible to strongly decrease the effect of the feed-through and to remain FCC compliant. Each device thus requires a tailor-made adjustment of the coupler in order to remove the effect of the feed-through.

IV. Construction of the IR-UWB Transmitter

The UWB transmitter is made in Duroid RO4003C, which is better suited than FR4 for high-frequency designs; its dielectric constant is $\varepsilon_r = 3.38$. The thickness h of the board is 0.508 mm (20 mil) and the thickness of the copper t is 35 μm after etching and gold plating. The transmission lines have the shielded microstrip (or coplanar waveguide with ground as in [11]) configuration (see Fig. 4) because it gives good protection against RF radiation and is also easy to include in the layout by simply drawing a ground plane around all RF tracks. For this configuration, the lines are sized by using the following formula (refer to [11] for more detail):

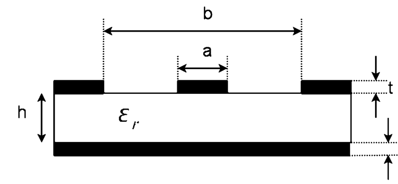

Fig. 4. Shielded microstrip configuration.

$$Z_0 = \frac{\eta_0}{2\sqrt{\varepsilon_{\text{eff}}}\left(\frac{K(k)}{K(k')} + \frac{K(k_1)}{K(k_1')}\right)}$$

with $k = (a/b) \quad k' = \sqrt{1-k^2} \quad k_1' = \sqrt{1-k_1^2}$ and

$$k_1 = \frac{\tanh\left(\frac{\pi a}{4h}\right)}{\tanh\left(\frac{\pi b}{4h}\right)} \quad \varepsilon_{\text{eff}} = \frac{1+\varepsilon_r \frac{K(k')}{K(k)}\frac{K(k_1)}{K(k_1')}}{1+\frac{K(k')}{K(k)}\frac{K(k_1)}{K(k_1')}}$$

where K is the complete elliptic integral of the first kind. The calculation gives (after several iterations) a width for the signal track of $a = 1.25$ mm and, by considering a gap between tracks of 120 μm that is the smallest resolution that can be achieved by our printed circuit board (PCB) workshop, a distance between grounds of $b = 1.25 + 2 \cdot 0.12 = 1.49$ mm in order to have a matching impedance of 50 Ω. Although a good design of the transmission lines and ground planes reduces significantly the radiated power of the circuit, the PCB should be packaged in a metal case with a screwed cover in order to completely shield the environment against the radiation coming mainly from the PLL synthesizer. It is important to use many vias to connect both top and bottom ground planes in order to have the least amount of parasitic inductance, especially near high-frequency signal tracks. The circuit is gold plated by electrochemical means in order to avoid corrosion of the copper that would rapidly degrade the performance. When components are soldered, the circuit is placed in the aluminium case and glued with a conductive glue (with silver) and placed in an oven for polymerisation for 3 h at 70 °C. The connection between the UWB transmitter and the outside world is made with SMA connectors for RF signals and through dc filters that are screwed into the shielding case for a dc power supply and tuning voltages. The microcontroller is then flashed with its software. The resulting circuit is shown in Fig. 5.

V. Measurement on the IR-UWB Transmitter

The signal produced by the UWB transmitter is shown in frequency (see Figs. 6 and 7) and in time (see Fig. 8) domains with a 1-MHz pseudorandom signal at the input. The signal has a power density of about −42.7 dBm/MHz at around 4.25 GHz and −51.3 dBm/MHz at 4.0 and 4.5 GHz, thus making the UWB transmitter compliant with the FCC rules (see Fig. 7). In the time domain, we see that the signal lasts approximately 3.2 ns and has an amplitude of around 400 mV$_{pp}$. We also see that the envelope of the signal is trapezoidal because of the balun.

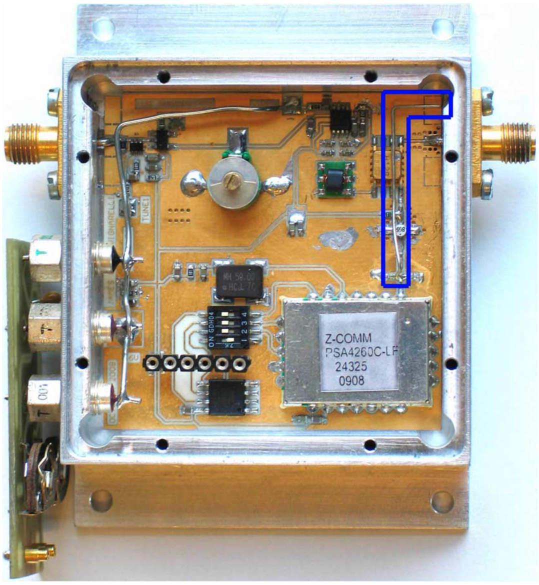

Fig. 5. Close view of the transmitter. The transmitter is made using Duroid RO4003C material. The square shape makes the circuit fit the RF shielding case in aluminium. The blue line (in online version) shows the transmission line coupler used to cancel the feed-through; its shape is obtained by experimentation.

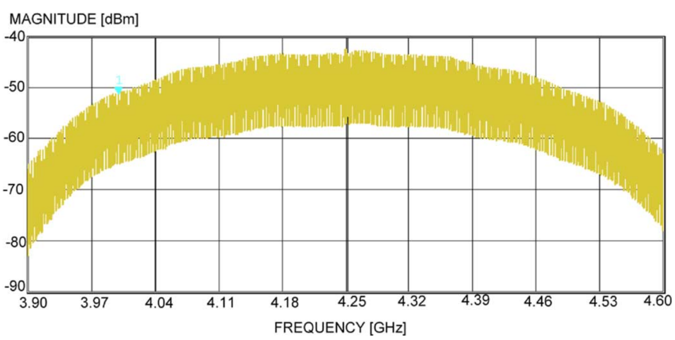

Fig. 6. Spectrum of the signal at the output of the UWB transmitter from 3.9 to 4.6 GHz.

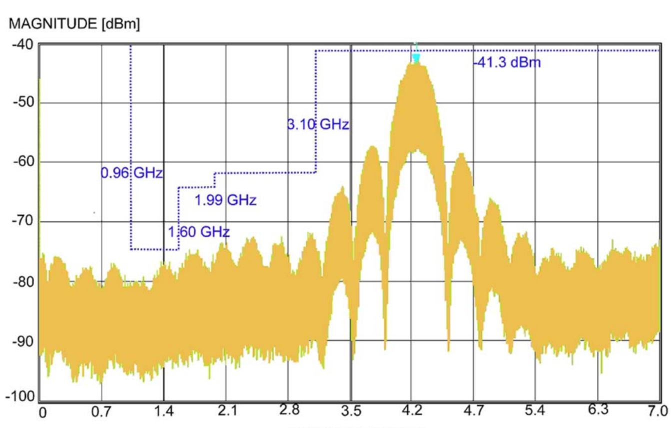

Fig. 7. Spectrum of the signal at the output of the UWB transmitter from dc to 7 GHz with the FCC regulations mask [3].

This trapezoidal shape increases the width of the UWB signal and decreases the intensity of the secondary lobes that would be higher with a pure rectangular envelope. The circuit is supplied with 5 V and has a current consumption of 132 mA; thus it has a power consumption of 660 mW, most of it used by the PLL, LO, monolithic microwave integrated circuit (MMIC) amplifier, and biasing resistors. This power consumption, although high, is acceptable in our case because the transmitter is intended to be used for measuring and testing purposes and not for real mobile low-power applications. We estimate that the consumption can be decreased to 570 mW—and thus save 90 mW—by using a switching power supply, instead of voltage drops across resistors, for delivering all the voltages required by the components of the transmitter.

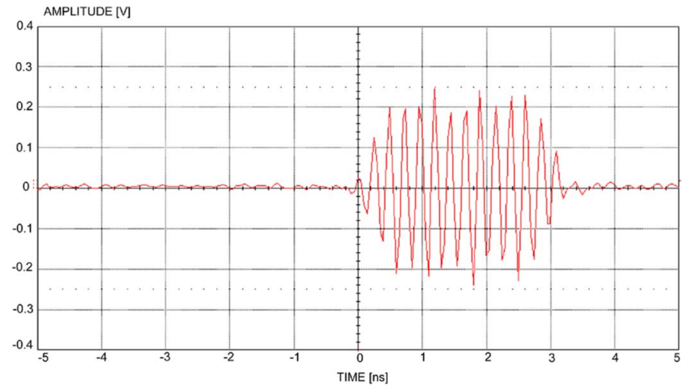

Fig. 8. Signal at the output of the UWB transmitter in the time domain.

TABLE I
LIST OF COMPONENTS USED FOR THE UWB TRANSMITTER

PLL oscillator	PCA 4260C-LF, Z-Comm
Microcontroller	ATTiny13, Atmel Corporation
"Slow" Comparator	ADCMP601, Analog Devices
"Fast" Comparator	ADCMP553, Analog Devices
Schmitt trigger inverter	NC7S14, Fairschild Semiconductor
Balun Transformer	CX2024, Pulse
Reference Oscillator	VX3@50MHz, Jauch Quartz
Switching mixer	HMC128, Hittite Corporation
Power amplifier MMIC	MGA-85576, Agilent
Duroid substrate	RO4003C, Rogers Corporation
Aluminium case	ZG3-2, Telemeter

VI. CONCLUSION

We have developed a generic system that is easy to use and to build for testing protocols and synchronization algorithms; its architecture is easy to modify for different central frequencies or bandwidths. In case the power consumption remains a problem, it is also easy to decrease it by 14% by using switching power supply ICs in place of resistors. In our case, the results of the experimental demonstration and validation of the IR-UWB transmitter completely fulfills the expectations and regulations, thanks to its tuning facilities.

APPENDIX
DETAILED LIST OF COMPONENTS

For a detailed list of components, please refer to Table I.

ACKNOWLEDGMENT

The authors would like to acknowledge J.-F. Zürcher, Ecole Polytechnique Fédérale de Lausanne (EPFL), Lausanne, Switzerland, who gave a lot of very valuable information about RF design and shielding techniques, J. Gerrits, Centre

Suisse d'Electronique et Microtechnique (CSEM), Neuchâtel, Switzerland, who suggests the use of a coupling line for attenuating the feed-through, Prof. J.-Y. Le Boudec, EPFL, for his scientific advice, as well as the workshops Ateliers de fabrication de Circuits Imprimés and Atelier de fabrication, de Conception, réalisation et Test (ACI and ACORT, EPFL) for their technical support and the quality of their work.

REFERENCES

[1] J. Colli-Vignarelli, J. Vernez, R. Merz, C. Dehollain, S. Robert, and J.-Y. Le Boudec, "Concurrent transmissions in IR-UWB networks: An experimental validation," in *Int. UWB Conf.*, Sep. 2009, pp. 337–342.

[2] H. Zhan, J. Ayadi, J. Farserotu, and J.-Y. Le Boudec, "Impulse radio ultra-wideband ranging based on maximum likelihood estimation," *IEEE Trans. Wireless Commun.*, vol. 8, no. 12, pp. 5852–5861, Dec. 2009.

[3] "First report and order: Revision of Part 15 of the Commission's rules regarding ultra-wideband transmission systems," FCC, Washington, DC, Govern. Printing Office Docket 98-153, Apr. 2002.

[4] J. Ryckaert, C. Desset, A. Fort, M. Badaroglu, V. De Heyn, P. Wambacq, G. Van der Plas, S. Donnay, B. Van Poucke, and B. Gyselinckx, "Ultra-wide-band transmitter for low-power wireless body area networks: Design and evaluation," *IEEE Trans. Circuits Syst. I, Reg. Papers*, vol. 52, no. 12, pp. 2515–2525, Dec. 2005.

[5] D. Wentzloff, R. Blazquez, F. Lee, B. Ginsburg, J. Powell, and A. Chandrakasan, "System design considerations for ultra-wideband communication," *IEEE Commun. Mag.*, vol. 43, no. 8, pp. 114–121, Aug. 2005.

[6] R. Fontana, "Recent system applications of short-pulse ultra-wideband (UWB) technology," *IEEE Trans. Microw. Theory Tech.*, vol. 52, no. 9, pp. 2087–2104, Sep. 2004.

[7] J. Moll and S. Hamilton, "Physical modeling of the step recovery diode for pulse and harmonic generation circuits," *Proc. IEEE*, vol. 57, no. 7, pp. 1250–1259, Jul. 1969.

[8] J. Han and C. Nguyen, "A new ultra-wideband, ultra-short monocycle pulse generator with reduced ringing," *IEEE Microw. Wireless Compon. Lett.*, vol. 12, no. 6, pp. 206–208, Jun. 2002.

[9] G. Quintero Diaz de Leon, A. Skrivervik, and J.-F. Zürcher, "Omnidirectional pulse dispersion of planar circular monopoles," in *Int. UWB Conf.*, Sep. 2009, pp. 395–399.

[10] M. Cavallaro, T. Copani, and G. Palmisano, "A gaussian pulse generator for millimeter-wave applications," *IEEE Trans. Circuits Syst. I, Reg. Papers*, vol. 57, no. 6, pp. 1212–1220, Jun. 2010.

[11] B. C. Wadell*, Transmission Line Design Handbook*. London, U.K.: Artech House, 1991, pp. 79–80.

James Colli-Vignarelli was born in Geneva, Switzerland, in 1978. He received the B.Sc. degree in mathematics from the University of Geneva, Geneva, Switzerland, in 2002, the M.Sc. degree in electrical engineering from the Ecole Polytechnique Federale de Lausanne (EPFL), Lausanne, Switzerland, in 2007, and is currently working toward the Ph.D. degree in IR-UWB transmitters at EPFL.

His research interests include RF CMOS circuit design and architecture for UWB applications.

Catherine Dehollain received the Electrical Engineering and Ph.D. degrees from the Ecole Polytechnique Federale de Lausanne (EPFL), Lausanne, Switzerland, in 1982 and 1995, respectively.

From 1982 to 1984, she was a Research Assistant with the Electronics Laboratories (LEG), EPFL. In 1984, she joined the Motorola European Center for Research and Development, Geneva, Switzerland, where she designed ICs applied to telecommunications. In 1990, she joined EPFL, as a Senior Assistant of the Chaire des Circuits et Systemes (CIRC), where she was involved in impedance broadband matching. Since 1995, she has been responsible at the RFIC Group, EPFL, for RF activities. She has been the Technical Project Manager of European projects, CTI projects, and Swiss National Science Foundation projects dedicated to RF wireless micropower sensor networks and mobile phones. Since 1998, she has been a Lecturer with EPFL, where she has been involved in the area of RF circuits, electric filters, and computer-aided design (CAD) tools. Since 2006, she has been a Maitre d'Enseignement et de Recherche (MER) with EPFL. She has authored or coauthoed four scientific books and 50 scientific publications. Her current research interests include low-power analog circuits, biomedical remotely powered sensors, and electric filters.